Neutron-Induced Signal on the Single Crystal CVD Diamond-Based Neutral Particle Analyzer

S. Kamio[1,a)], Y. Fujiwara[1], K. Ogawa[1,2], M. I. Kobayashi[1], S. Sangaroon[1], M. Isobe[1,2], R. Seki[1,2], H. Nuga[1], M. Osakabe[1,2], S. Matsuyama[3], M. Miwa[3], and S. Toyama[3]

[1]*National Institute for Fusion Science, 322-6 Oroshi-cho, Toki 509-5292, Japan*
[2]*The Graduate University for Advanced Studies SOKENDAI, 322-6 Oroshi-cho, Toki 509-5292, Japan*
[3]*Tohoku University, 6-6 Aoba, Aramaki, Aoba-ku, Sendai 980-8579, Japan*

(Received XXXXX; accepted XXXXX; published online XXXXX)

The diamond-based neutral particle analyzer (DNPA) array composed of single-crystal chemical vapor deposition (sCVD) diamond detectors was installed on the Large Helical Device (LHD) for measuring the helically-trapped energetic particles. In the high neutron flux experiment, the unwanted neutron-induced pulse counting rate should be estimated using the other neutron diagnostics because a diamond detector has sensitivity to neutron as well as energetic neutral particles. In order to evaluate the quantitative neutron-induced pulse counting rate on DNPA, the response functions of the sCVD diamond detector for mono-energetic neutrons were obtained using accelerator-based D-D and D-^{7}Li neutron sources in Fast Neutron Laboratory (FNL). As the result of the neutron flux estimation by Monte Carlo N-Particle (MCNP) code at the NPA position in LHD and the response function obtained in FNL experiment, the counting rate of the neutron-induced signal was predicted to be 2.3 kcps during the source neutron emission rate S_n=1x10^{15} n/s. In the LHD experiment, the neutron-induced signals were observed by closing the gate valve during the plasma discharges. It is found that the counting rates of the neutron-induced signals proportional to S_n reached 1.1 kcps at S_n=1x10^{15} n/s. As the result of the quantitative estimation of the neutron-induced signals on DNPA using other neutron measurement, it has become possible to accurately measurement of energetic neutral particles in the high neutron flux experiment.

I. INTRODUCTION

In the future fusion reactor, alpha particles should be well confined and used for plasma heating to sustain steady-state without external heating. Therefore, it is very important to study the confinement physics of energetic particles because the energetic particles can cause magnetohydrodynamic (MHD) instabilities which transport the energetic particles, and deteriorate the confinement of the energetic particles. In order to investigate the behavior of the energetic particles in the experimental devices for fusion research, neutral particle analyzer (NPA) has been developed [1]. The energy spectrum of the energetic particles which charge exchanged inside the plasma can be observed by NPA along the line of sight. silicon-diode detector is widely used because of the good energy resolution and a size small enough to make an array [2-6]. However, high neutron irradiation causes a permanent damage on the semiconductor products, such as silicon-diode-based NPA. Since the silicon-diode detector cannot be used in burning plasma, diamond detector which has sufficient neutron radiation hardness has been developed [7,8]. On the other hand, in the experiment using deuterium gas, the neutron emission produced by the D-D fusion reaction is also used for investigating the behavior of the energetic particles because the neutron emission rate depends on the spatial and energy distribution functions of energetic particles. Therefore, by measuring the energetic particles in the hard neutron radiation experiments, comprehensive investigation can be done together with the neutron measurement. The result of the NPA is useful because the energy spectrum of the energetic particles can be obtained.

In the Large Helical Device (LHD), confinement of the energetic particles in a helical ripple is studied for understanding the confinement physics in three-dimensional magnetic configuration because the transport of the helically trapped energetic particles is one of the important issues for the helical confinement system. In LHD, the deuterium plasma experiment has been started in FY 2016, and the neutron diagnostics are installed for the study of the energetic particles by D-D fusion reaction [9,10]. In order to measure the energetic particles in the hard neutron radiation experiment, single-crystal chemical vapor deposition (sCVD) diamond-based NPA (DNPA) was developed for measuring the helically trapped energetic particles in LHD [11]. The diamond was adopted because of its high radiation hardness. Using the DNPA, energy spectra of the energetic particles were observed with high energy resolution in the high neutron emission experiments. By measuring in the high neutron emission experiment, DNPA can be used together with the neutron diagnostics [12,13] as well as the other NPAs [14,15] and spectroscopic measurements [16,17]. DNPA also detects the neutron-induced signals during the discharge in the deuterium experiment. However, the quantitative neutron-induced signals on the DNPA have not been evaluated yet. As the diagnostic for

[a)]Author to whom correspondence should be addressed: kamio@nifs.ac.jp.

the energetic neutral particle, the neutron-induced signals should be estimated from the neutron measurement.

In this paper, we show the results of the neutron-induced signals on the sCVD diamond detectors for NPA. The DNPA system configuration is shown in the Section II. The Section III shows the observed energy spectra by the neutron irradiation experiments in Fast Neutron Laboratory (FNL). Quantitative evaluation of neutron-induced signal on diamond detector was observed in FNL. In Section IV, the results in the LHD experiments are shown. The neutron-induced signal on DNPA was measured experimentally. Also, the typical experimental results are shown with the neutron-induced signal estimation. Section V is summary.

II. DNPA SYSTEM CONFIGURATION

The schematic view of the circuit of the DNPA is shown in Fig. 1. The sCVD diamond B12 [18], made by CIVIDEC, is used for the detector of the DNPA [11]. The sCVD diamond is 4.5 mm x 4.5 mm with 0.5 mm thickness, and the electrode is 4.0 mm x 4.0 mm with 100 nm thickness made of titanium. In the case for the plasma diagnostics in fusion research, one of the target beam energies is 40-80 keV which is the typical energy of the positive ion source neutral beam injection (NBI). In order to measure the 40-80 keV energy signals, the electrodes were customized to the thinner titanium from the gold electrodes, and the preamplifier 2001A and the shaping amplifier 2026X which are made by CANBERRA were used to achieve high multiplication. Typical magnification at the amplifier is 750 times, and the shaping time is 0.2 μs. The corresponding energy of the thermal noise was less than approximately 30 keV. Therefore, the typical energy range of the DNPA is 30-600 keV. For acquiring energy calibration data, ^{241}Am alpha source was used. The digitizer WE7562 for pulse height analysis made by YOKOGAWA is used for counting the signals. The pulse length of the signal is approximately 1 μs in the counting time window of 10 ms. Therefore, in order to avoid the pile-up, DNPA should be used with the counting rate of less than 100 kcps. The counting loss rate due to the dead-time of the detector [19] is 10% of the true count under 100 kcps.

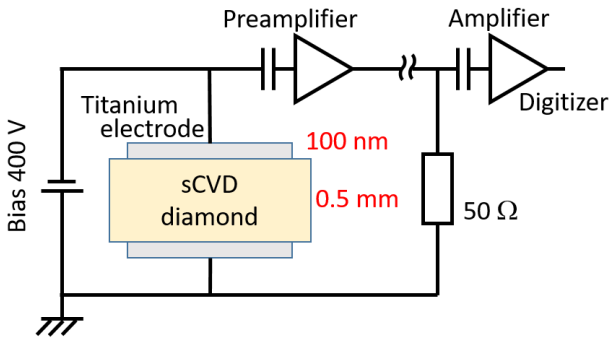

Fig. 1 The schematic view of the circuit of the DNPA.

III. NEUTRON IRRADIATION IN FNL

In order to measure the quantitative neutron-induced signal on DNPA, fast neutron irradiation experiments have been demonstrated in Fast Neutron Laboratory (FNL) [20,21] at Tohoku University. Figure 2 shows the schematic view of the FNL experiments. The accelerated deuteron DC beam by the Dynamitron accelerator is delivered to the target with the energy of E_{beam}. The deuterium gas or the solid lithium was used as a target. The neutrons produced by D(d,n)^{3}He or by ^{7}Li(d,n)^{8}Be reactions were detected at the sCVD diamond detector with the energy of E_n+E_{beam}cosα. E_n of 2.45 MeV with D(d,n)^{3}He reaction was used for evaluating the neutron-induced signals in D-D fusion plasma experiment, and E_n of 15.0 MeV with ^{7}Li(d,n)^{8}Be reaction was used for measuring the neutrons by DNPA.

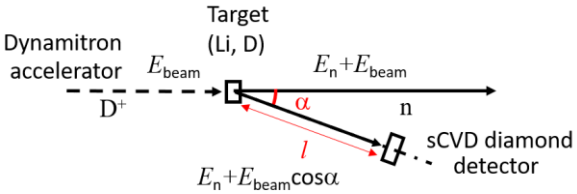

Fig. 2 Schematic view of the FNL experiments.

The deuterium gas target was used for measuring the neutron counting rate by 2.45 MeV D-D fusion reaction. The detector was installed at l=35 mm and α=20 deg. 20 m cables for connecting the amplifiers were used for reproducing the experimental conditions. Figure 3 shows the energy distributions of the DNPA counting rate during the neutron irradiation experiment. The irradiated neutron energy was 3.57-5.52 MeV with the acceleration voltage of 2.1-3.0 MV. The neutron irradiation time was 20 minutes for each energy. The observed counting rate divided by the neutron flux rate was approximately 4.6x10^{-4} count/n with the energy range of 50-600 keV. A characteristic peak was observed at 200-300 keV. This peak is the elastic scattering of the neutrons on ^{12}C nucleus. The amplitude and energy of the peak were changed by changing the irradiated neutron energy. The irradiation neutron energy dependency on the DNPA counting rate was not clear in this energy range. The calculation of elastic scattering inside the diamond due to the neutron irradiation by PHITS code [22] also shows the similar result. Therefore, we consider the energy spectrum of DNPA due to the neutron irradiation with the energy of 2.45 MW is almost same with the spectra shown in Fig. 3.

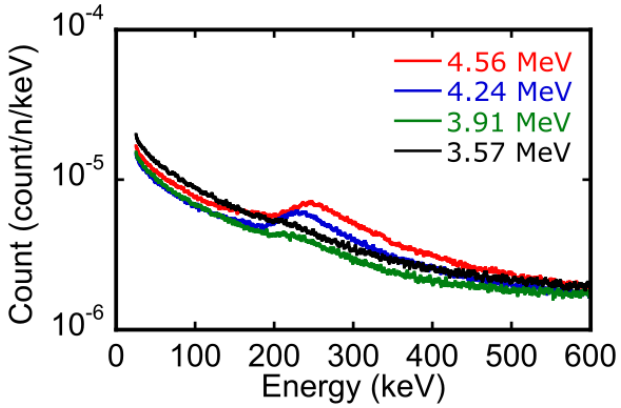

Fig. 3 The energy distributions of the DNPA counting rate of the neutron irradiation experiments using D-D neutron source.

Figure 4 shows the results of the experiment with D-^{7}Li neutron source, measured with the wide energy range. By decreasing the magnification of the amplifier to 50 times, the error by the thermal noise was decreased. The irradiated neutron energies were 15.89 MeV, 16.99 MeV, and 17.68 MeV with the acceleration voltage of 1.5 MV, 2.4 MV, and 3.0 MV, respectively. As the result of the neutron irradiation, characteristic energy distributions were observed. The peaks of ^{12}C(n,α)^{9}Be and ^{12}C(n,n')3α could be identified by DNPA.

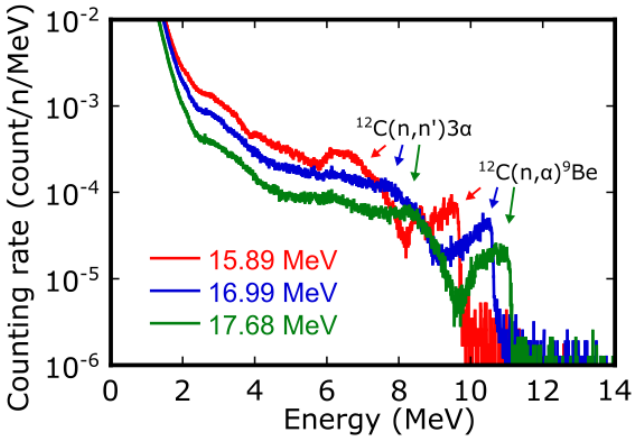

Fig. 4 The energy distributions of the DNPA counting rate of the neutron irradiation experiments using D-^{7}Li neutron source.

IV. EXPERIMENTS IN LHD

In LHD, DNPA was developed for measuring the energetic particles which were accelerated by ion cyclotron range of frequency (ICRF) wave or injected by perpendicular-neutral beam (p-NB) injectors. The DNPA measurement lines of sight with the LHD poloidal cross-section are shown in Fig. 5. The lines of sight of Ch1 and of Ch7 are across the lower and upper helical ripple, and line of sight of Ch4 is across the magnetic axis. Because the direction of the measurement lines of sight are perpendicular to the magnetic field lines, Ch1 and Ch7 are expected to observe the helical ripple trapping particles. The DNPA counting rate is expected to be high during the p-NB injection. On the other hand, neutron emission rate is high during the tangential-neutral beam (t-NB) injection because the injection energy of the t-NBs is higher than the injection energy of p-NBs. The typical injection energy of t-NB (NB #1, #2 and #3) is 130-180 keV, and the typical injection energy of p-NB (NB #4 and #5) is 60-80 keV.

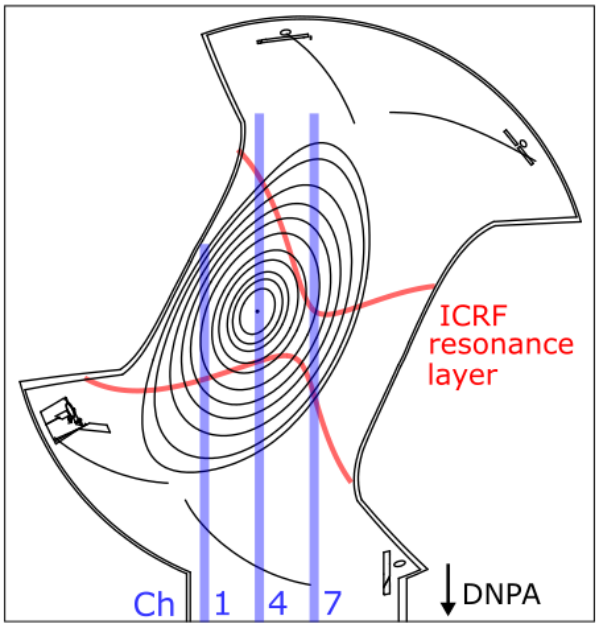

Fig. 5 The lines of sight of DNPA together with the plasma flux surface and the ICRF resonance layers in the LHD poloidal cross-section.

The diamond detectors were installed at the basement of the LHD torus hall. Three meter straight pipes were used to extend the vacuum chamber from LHD lower side port. In order to reduce the neutron effect, the diamond detectors are located under the floor slab through 1.5 m heavy concrete with 5 cm inner diameter pipes. The detectors are located at approximately 7.8 m lower from the magnetic axis of the torus plasma. The neutron flux was calculated by Monte Carlo N-Particles transport (MCNP) code [23,24]. The neutron flux at the position of the detectors were evaluated approximately 5x10^{6} n/cm^{2}/s when the neutron source emission rate is 1x10^{15} n/s [25]. The neutron source emission rate S_n is measured by the neutron flux monitor [26]. Considering the estimatated counting rate 4.6x10^{-4} count/n with the energy range of 50-600 keV in the FNL experiment in Fig. 3, the predicted counting rate by S_n is approximately 2.3 kcps during the LHD experiment with S_n=1x10^{15} n/s.

Figure 6 shows the experimental result of the neutron-induced signal measurement. During the discharges with the high neutron emission rate, DNPA measured the signals other than the neutral particles by closing gate valve. The gate valve which is made of stainless steel prevents passing through energetic neutral particles. 49 discharges with high S_n rate of up to 2.5x10^{15} n/s were used for neutron-induced signal measurement. As shown in Fig. 6 (a), the energy integrated neutron signals were clearly proportional to S_n. The counting rate coefficients of three DNPA channels were almost the same. As the result of the linear fitting, the DNPA average counting rate for S_n was 1.1 kcps when S_n=10^{15} n/s. Observed counting rate 1.1 kcps was close to the prediction i.e. 2.3 kcps. This result also indicates that the calculation of the neutron flux rate at the basement by MCNP of 5x10^{6} n/cm^{2}/s at S_n=10^{15} n/s was reasonable. The energy distributions of each channel are shown in Fig. 6 (b). A peak of neutron-induced signal shape similar to the result in FNL

experiment shown in Fig. 3 was observed at around 300 keV. These results can be used for estimation of the counting rate of the neutron-induced signal during the neutral particle measurement.

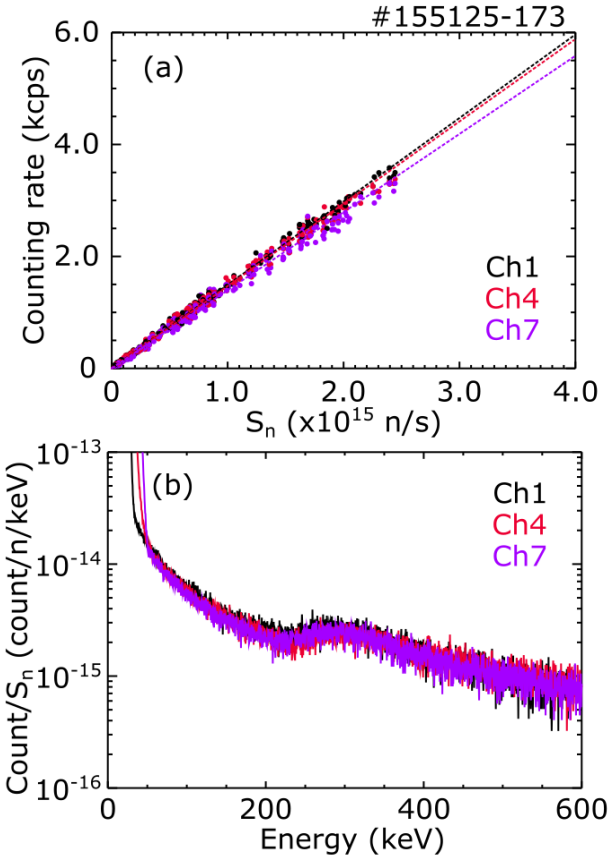

Fig. 6 (a) The DNPA integrated counting rates of 50-600 keV during the discharges with the gate valve closed. (b) The energy distributions of each channel. The counting rates are normalized by 10^{15} neutrons.

Typical experimental results measuring the energetic neutral particles in LHD are shown in Figs. 7 and 8. Fig. 7 (a) shows the time evolutions of injection powers, Fig. 7 (b) shows the plasma density and the temperatures, and Fig. 7 (c) shows the total neutron emission rate S_n. In this discharge, p-NB and t-NB are used as the energetic particle source, and ICRF heating is used to accelerate ions. The highest S_n is 1.1x10^{15} n/s at the timing of t-NB injection. Figs. 7 (d)-(f) are the energy integrated counting rates of the DNPA (red) and the estimated neutron-induced signal (yellow) of each channel. The highest counting rate was less than 30 kcps at the timing of p-NB injection. The p-NB modulation pulses, which were injected with the energy of 59 keV, can be clearly confirmed on DNPA Ch1 and Ch7. On the other hand, the counting rate of Ch4 was lower than the counting rate of Ch1 and of Ch7. This difference indicates that the p-NB particles were trapped in a helical ripple. In the case of Ch4, the counting rate was close to the estimation of the counting rate of neutron-induced signal. The total counting rate of Ch1 was higher than the counting rate of Ch7 during the p-NB injection. However, during the timing of ICRF injection of 5.3-6.3 s, the counting rate of Ch7 was higher than that of Ch1. This count of Ch7 may be the accelerated particles at the ICRF resonance layers on the Ch7 line of sight shown in Fig. 5. The estimated neutron-induced signal of this timing was negligible.

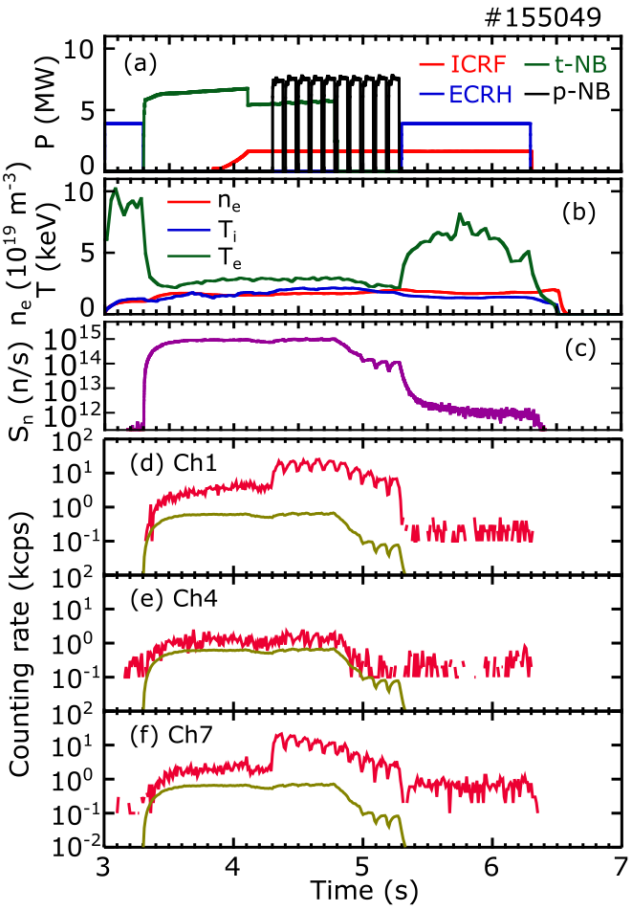

Fig. 7 Time evolutions of (a) the injection powers for plasma start-up, sustaining and heating, (b) the electron density and the temperatures of ion and electron, (c) the total neutron emission rate, and (d)-(f) the counting rates of the DNPA each channel at 50-300 keV (red) and the estimated neutron-induced signal (yellow).

The energy distributions of the discharge are shown in Fig. 8. Red lines are the total count during 3-7 seconds shown in Fig. 7. Black lines are thermal noise estimated before the plasma start-up in the same discharge. Yellow lines are the estimated spectra of the neutron-induced signal using the energy distributions of Fig. 6 (b). The counting rate of the neutral particles were much higher than the neutron-induced signal at the lower energy region. However, the neutral counting rate was almost the same with the neutron-induced signal at more than 100 keV, 70 keV, and 90 keV for Ch1, Ch4, and Ch7, respectively. The estimation of the neutron noise was very important for discussing the confinement of energetic particles in the high energy region.

The higher energy components than the p-NB energy of 59 keV are considered to be the scattered t-NB particles which were injected with the energies of 153 keV (NB #1), 170 keV (NB #2),

and 170 keV (NB #3), or the accelerated particles by ICRF heating. We will clarify the confinement physics generated by p-NB injection and/or ICRF heating using DNPA by changing the experimental conditions in the LHD.

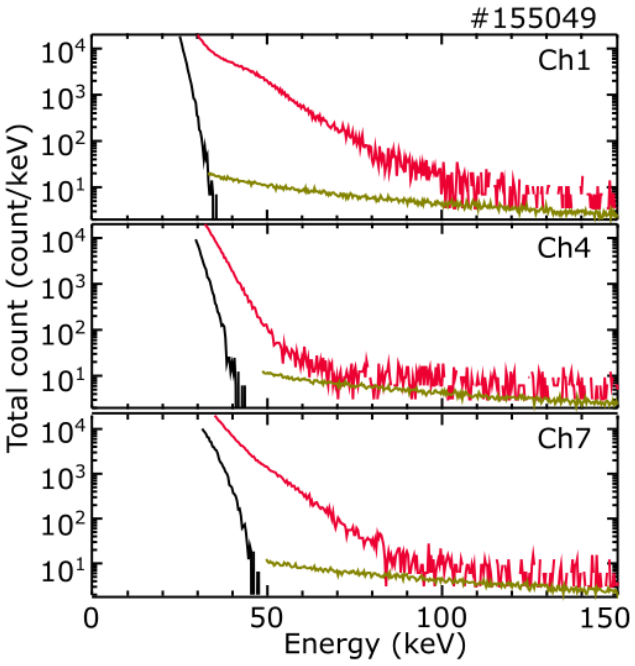

Fig. 8 Energy spectra of the total count (red), the estimated neutron-induced signal (yellow), and the thermal noise (black) of each channel.

V. SUMMARY

The NPA array using sCVD diamond detectors was developed in the LHD deuterium experiments for measuring the helically trapped energetic particles. In order to measure the quantitative neutron-induced signals on the DNPA, mono-energetic neutron was irradiated to the sCVD diamond detector in FNL. As the result of the FNL experiments and the neutron flux estimation by MCNP, the neutron-induced signal was estimated to be 2.4 kcps during plasma discharges with the total neutron emission rate S_n=10^{15} n/s in LHD. This counting rate is low enough to measure the neutral particles without the pile-up due to the neutron-induced signal. The characteristic peak was observed at around 200 keV, and the peak was shifted by changing the energy of irradiated neutron. The characteristic energy spectra of fast neutron signals were also observed by diamond detectors with wide energy range in FNL experiment. In LHD, the neutron-induced signals were measured by closing the gate valve during the plasma discharges. The amount of the signals due to the neutron result in a linear relation with the neutron emission. The counting rate of the neutron-induced signal was 1.1 kcps when S_n=10^{15} n/s. This counting rate is a similar value to the prediction. Using the results of the neutron measurement, the neutron-induced signal was estimated quantitatively during the experiment for measuring the energetic neutral particles. The counting rate due to neutrons were estimated to be much lower than the signal of the neutral particles even during the neutron emission rate of 10^{15} n/s, which is the highest neutron emission rate in LHD experiments.

DATA AVAILABILITY

The data that support the findings of this study are available from the corresponding author upon reasonable request.

ACKNOWLEDGMENTS

The authors wish to thank the support of the LHD experiment group in performing the experiments. This work is supported by the NINS program for cross-disciplinary study (Grant No. 0131190), the NIFS Collaboration Research Program (KOAH037, KOAA001), and the NIFS Grants (ULRR006, ULRR035, and ULRR703).

[1]D. D. R. Summers, R. D. Gill and P. E. Stott, J. Phys. E: Sci. Instrum. **11** (1978) 1183.
[2]Y. Miura, H. Takeuchi, and Y. Ohara, Rev. Sci. Instrum. **56** (1985) 1111.
[3]M. Osakabe, T. Yamamoto, Y. Takeiri, T. Mutoh, E. Asano, K. Ikeda, K. Tsumori, O. Kaneko, K. Kawahata, N. Ohyabu *et al*., Rev. Sci. Instrum. **72** (2001) 788-791.
[4]V. Tang, J. Liptac, R. R. Parker, P. T. Bonoli, C. L. Fiore, R. S. Granetz, J. H. Irby, Y. Lin, S. J. Wukitch, The Alcator C-Mod Team *et al*., Rev. Sci. Instrum. **77** (2006) 083501.
[5]J. Kalliopuska, F. García, M. Santala, S. Eränen, S. Karttunen, T. Virolainen, T. Kovero, T. Vehmas, R. Orava, Nucl. Instrum. Methods Phys. Res A **591** (2008) 92-97.
[6]S. H. Kim, J. G. Kwak, C. K. Hwang, S. J. Wang, H. J. Lee, Fusion Eng. Des. **86** (2011) 1236-1238.
[7]M. Isobe, Y. Kusama, M. Takechi, T. Nishitani, and A. Morioka, Rev. Sci. Instrum. **72** (2001) 611.
[8]A. G. Alekseyev, D. S. Darrow, A. L. Roquemore, and S. S. Medley, Rev. Sci. Instrum. **74** (2003) 1905.
[9]K. Ogawa, M. Isobe, T. Nishitani, S. Murakami, R. Seki, H. Nuga, S. Kamio, Y. Fujiwara, H. Yamaguchi, Y. Saito *et al*., Nucl. Fusion **59** (2019) 076017.
[10]H. Nuga, R. Seki, K. Ogawa, S. Kamio, Y. Fujiwara, M. Osakabe, M. Isobe, T. Nishitani, M. Yokoyama, and LHD Experiment Group, Plasma Fusion Res. **14**, 3402075 (2019).
[11]S. Kamio, Y. Fujiwara, K. Ogawa, M. Isobe, R. Seki, H. Nuga, T. Nishitani, M. Osakabe and the LHD Experiment Group, JINST **14**, C08002 (2019).
[12]M. Isobe, K. Ogawa, T. Nishitani, H. Miyake, T. Kobuchi, N. Pu, H. Kawase, E. Takada, T. Tanaka, S. Li *et al*., IEEE Trans. Plasma Sci. **46** (2018) 2050-2058.
[13]K. Ogawa, M. Isobe, T. Nishitani, S. Murakami, R. Seki, H. Nuga, S. Kamio, Y. Fujiwara, H. Yamaguchi, Y. Saito *et al*., Nucl. Fusion **59** (2019) 076017.
[14]Y. Fujiwara, S. Kamio, K. Ogawa, H. Yamaguchi, R. Seki, H. Nuga, T. Nishitani, M. Isobe and M. Osakabe, JINST **15**, C02021 (2020).
[15]T. Ozaki, P. Goncharov, E. Veshchev, N. Tamura, S. Sudo, T. Seki, H. Kasahara, Y. Takase, and T. Ohsako, Rev. Sci. Instrum. **79** (2008) 10E518.
[16]Y. Fujiwara, S. Kamio, H. Yamaguchi, A. V. Garcia, L. Stagner, H. Nuga, R. Seki, K. Ogawa, M. Isobe, M. Yokoyama, *et al*., Plasma Fusion Res. **14**, 3402129 (2019).
[17]Y. Fujiwara, S. Kamio, H. Yamaguchi, A. V. Garcia, L. Stagner, H. Nuga, R. Seki, K. Ogawa, M. Isobe, M. Yokoyama *et al*., Nucl. Fusion (submitted).
[18]CIVIDEC Instrumentation GmbH. Austria, https://cividec.at/.
[19]J. W. Müller, Nucl. Instrum. Methods, **112**, (1973) 47-57.
[20]M. Baba, M. Takada, T. Iwasaki, S. Matsuyama, T. Nakamura, H. Ohguchi, T. Nakao, T. Sanami, N. Hirakawa, Nucl. Instrum. Methods Phys. Res. A **376**, (1996) 155-123.

[21]M. Sasaki, T. Nakamura, N. Tsujimura, O. Ueda, T. Suzuki, Nucl. Instrum. Methods Phys. Res. A **418** (1998) 465-475.
[22]T. Sato, Y. Iwamoto, S. Hashimoto, T. Ogawa, T. Furuta, S. I. Abe, T. Kai, P. E. Tsai, N. Matsuda, H. Iwase *et al*., J. Nucl. Sci. Technol. **55, 684-690** (2018).
[23]MCNP6 Users Manual, LA-CP-13-00634, in : D.B. Pelowits (Ed.), Los Alamos National Laboratory, Los Alamos, 2013.
[24]T. Nishitani, K. Ogawa, M. Isobe, Fusion Eng. Des. **123** (2017) 1020-1024.
[25]S. Sangaroon, K. Ogawa, M. Isobe, M. I. Kobayashi, Y. Fujiwara, S. Kamio, R. Seki, H. Nuga, H. Yamaguchi, M. Osakabe and LHD Experiment Group, Rev. Sci. Instrum. (submitted).
[26]M. Isobe, K. Ogawa, H. Miyake, H. Hayashi, T. Kobuchi, Y. Nakano, K. Watanabe, A. Uritani, T. Misawa, T. Nishitani *et al*., Rev. Sci. Instrum. **85** (2014) 11E114.